Hindawi Publishing Corporation
International Journal of Photoenergy
Volume 2009, Article ID 374301, 7 pages
doi:10.1155/2009/374301

Research Article

Impedance and Interface Properties of Al/Methyl-Red/*p*-InP Solar Cell

Ömer Güllü

Department of Physics, Science and Art Faculty, Batman University, 72060 Batman, Turkey

Correspondence should be addressed to Ömer Güllü, omergullu@gmail.com

Received 17 April 2009; Accepted 8 July 2009

Recommended by Fahrettin Yakuphanoglu

An Al/methyl-red/*p*-InP solar cell was fabricated via solution-processing method and was characterized by using current-voltage (*I-V*) and capacitance-voltage-frequency (*C-V-f*) measurements at room temperature. From dark *I-V* characteristics, the values of ideality factor and barrier height of the device were calculated as 1.11 eV and 2.02, respectively. It has been seen that the device exhibited a good photovoltaic behavior with a maximum open circuit voltage V_{oc} of 0.38 V and short-circuit current I_{sc} of 2.8 nA under only 200 lx light intensity. The barrier height and acceptor carrier concentration values for the Al/methyl-red/*p*-InP devices were extracted as 1.27 eV and 3.46×10^{17} cm^{-3} from linear region of its C^{-2}-V characteristics, respectively. The difference between Φ_b (*I-V*) and Φ_b (*C-V*) for Al/methyl-red/*p*-InP device was attributed the different nature of the *I-V* and *C-V* measurements. Also, the energy distribution curves of the interface states and their time constants were obtained from the experimental conductance properties of the Al/methyl-red/*p*-InP structure at room temperature. The interface state densities and their relaxation times of the device have ranged from 2.96×10^{12} cm^{-2}eV^{-1} and 4.96×10^{-6} s at (1.11-E_v) eV to 5.19×10^{12} cm^{-2} eV^{-1} and 9.39×10^{-6} s at (0.79-E_v) eV, respectively. It was seen that both the interface state density and the relaxation time of the interface states have decreased with bias voltage from experimental results.

1. Introduction

Over the last two decades, organic thin-film devices, such as organic light-emitting diodes, organic thin-film transistors, photodetectors, and solar cells, have made steady progress in device performance with ever increasing range of applications [1]. By many workers [2–20], it has been carried out their fabrications and electrical/optical characterizations of solar cells by using organic semiconductors. Organic semiconductors show many unusual electrical, optical, and magnetic properties, which could be used for the fabrication of molecular electronic devices [21]. These materials also offer low cost and processing ease and can attain new roles not realized by conventional solar cells [1, 4, 13, 14]. This has opened a new possibility of replacing conventional inorganic devices by the organic ones [21]. Among those, methyl-red is considered a good candidate for organic semiconductor device fabrication such as photoelectric converters and solar cells. Methyl-red with molecular formula NC_6H_4COOH (2-[4-(dimethylamino)phenylazo] benzoic acid) used in this study is a typical aromatic azo compound. Its colour originates from absorbance in the visible region of the spectrum due to the delocalization of electrons in the benzene and azo groups forming a conjugated system. Due to its conjugated structure and richness in 16 π electrons, the methyl-red has been chosen to form an organic semiconductor layer between Al and *p*-InP inorganic semiconductor substrate [22]. The molecular structure of the methyl-red is given in Figure 1(a). The structure of azo dyes has attracted considerable attentions recently due to their wide applicability in the light-induced photo isomerization process and their potential usage for the reversible optical data storage [8, 22, 23].

Our aim is to investigate the electrical properties of Al/methyl-red/*p*-InP solar cell by the insertion of methyl-red organic layer between InP semiconductor and Al metal by using and current-voltage (*I-V*) and capacitance-voltage-frequency (*C-V-f*) measurements in dark and is to compare the electrical parameters of the Al/methyl-red/*p*-InP solar cell with those of conventional Metal/Semiconductor diodes.

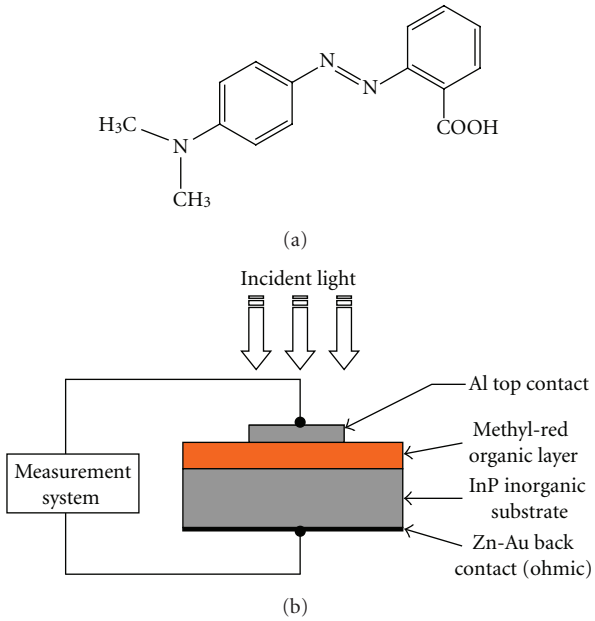

Figure 1: (a) Molecular structure of the methyl-red organic compound. (b) (Color online) The experimental setup of the Al/methyl-red/*p*-InP Schottky solar cell for the electrical and photovoltaic characterization.

Also, this work presents the physics of the photovoltaic device and describes the process of manufacturing and electrical characterization of organic-based solar cell exhibiting the photovoltaic properties.

2. Experimental Details

The organic/inorganic semiconductor (OI) photovoltaic device was prepared using one side polished (as received from the manufacturer) *p*-type InP wafer with $3.46 \times 10^{17}\,\text{cm}^{-3}$ doping density [8] from *C-V* measurements in this study. The wafer was chemically cleaned with $3H_2SO_4 + H_2O_2 + H_2O$ (a 20 seconds boiling). The native oxide on the front surface of *p*-InP was removed in an HF : H_2O (1 : 10) solution for 30 seconds, and finally the wafer was rinsed in deionized water. Before forming the organic layer on the *p*-InP substrate, the ohmic contact was made by evaporating Au-Zn (90%–10%) alloy on the back of the substrate, followed by a temperature treatment at 450°C for 3 minutes in a N_2 atmosphere. After the cleaning procedures and ohmic metallization, the methyl-red film on the front surface of the *p*-InP wafer was directly formed by methyl-red solution (wt 0.2% in methanol) by using the solution processing method. The contacting metal dots were formed by evaporation of Al dots with diameter of 1.0 mm. All evaporation processes were carried out in a vacuum coating unit at about 10^{-5} mbar. *I-V* and *C-V-f* measurements have been measured using a Keithley 487 Picoammeter/Voltage source and a HP 4192A LF Impedance Analyzer, respectively (see Figure 1(b)). A light source consisting of a halogen lamp was used for the *I-V* measurement under illumination.

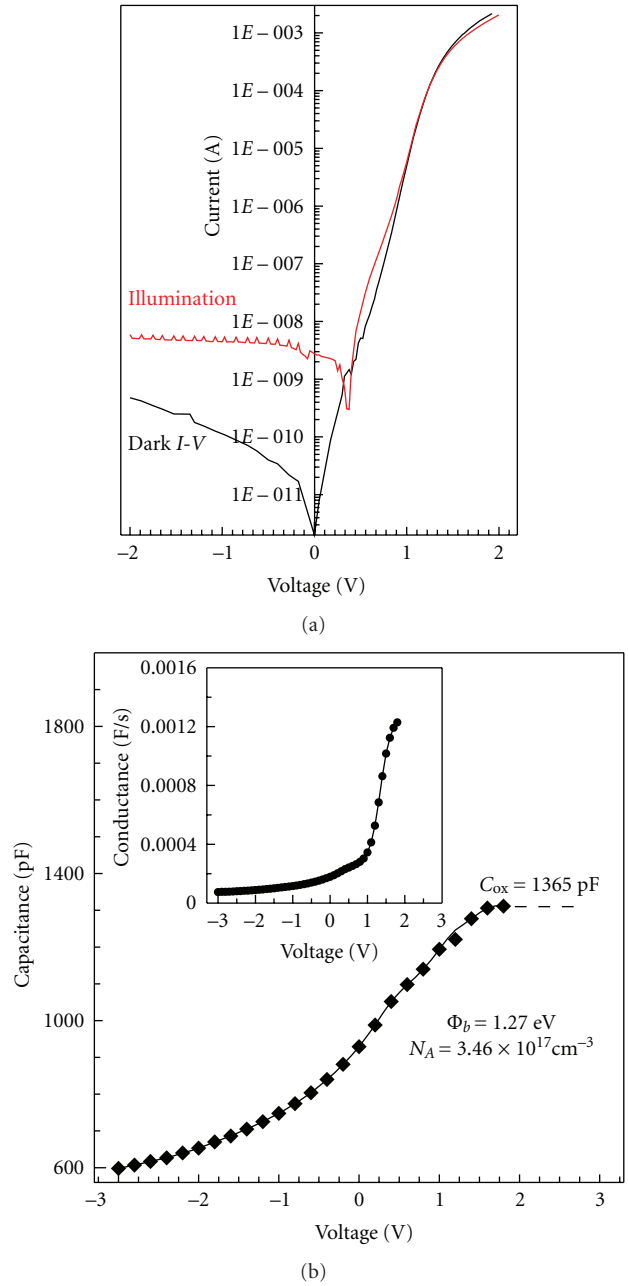

Figure 2: (a) (Color online) Semilog *I-V* characteristics of the Al/methyl-red/*p*-InP Schottky solar cell under dark (in black) and illumination (in red) conditions. (b) The *C-V* characteristic of the Al/methyl-red/*p*-InP solar cell in dark (inset depicts conductance-voltage characteristic obtained from the experimental *C-V* measurement).

3. Results and Discussion

3.1. The Photovoltaic Properties of the Al/Methyl-Red/p-InP Structure. Figure 2(a) shows experimental semilog *I-V* characteristics of the Al/methyl-red/*p*-InP OI Schottky device under dark (in black) and illumination (in red) conditions at room temperature. As clearly seen from Figure 2(a), the Al/methyl-red/*p*-InP OI diode represents

a good rectifying property. The weak voltage dependence of the reverse-bias current and the exponential increase of the forward-bias current are characteristic properties of rectifying interfaces. The current curve in forward bias quickly becomes dominated by series resistance from contact wires or bulk resistance of the organic material and inorganic semiconductor, giving rise to the curvature at high current in the semilog *I–V* plot. According to the thermionic emission theory [24, 25], the ideality factor n and barrier height (BH) Φ_b can be obtained from the slope and the current axis intercept of the linear regions of the forward bias *I-V* plots, respectively. The values of the Φ_b and the n for the Al/methyl-red/*p*-InP OI diode in dark have been calculated as 1.11 eV and 2.02, respectively. The ideality factor determined by the image-force effect alone should be close to 1.01 or 1.02 [26–28]. Our data clearly indicate that the diode has the ideality factor that is significantly larger than this value. Higher values of ideality factors are attributed to secondary mechanisms which include interface dipoles due to interface doping or specific interface structure (native oxide layer and methyl-red layer) as well as fabrication-induced defects at the interface [26–29]. According to Tung et al. [28], the high values of n can be attributed to the presence of a wide distribution of low-BH patches caused by laterally barrier inhomogeneous. Also, the image-force effect, recombination-generation, and tunneling may be possible mechanisms that could lead to an ideality factor value greater than unity [24, 28]. The obtained BH value for the Al/methyl-red/*p*-InP contact is different from a value of 0.83 eV [8] (from the *I-V* characteristic of reference diode) obtained for Al/*p*-InP metal/semiconductor structure. These findings indicate the methyl-red organic thin film formed on inorganic substrate that the barrier height of metal/semiconductor Schottky diodes changed in significant rate. The case may be attributed to an organic interlayer modifying the effective barrier height by influencing the space charge region of the inorganic substrate [17, 30]. Thereby, it is known that the organic film forms a physical barrier between metal and InP substrate, preventing the metal from directly contacting the InP surface [8–11, 15–19, 30]. The methyl-red organic layer appears to cause a significant modification of interface states even though the organic/inorganic interface becomes abrupt and unreactive [8–11, 15–19, 30]. Thus, the change in barrier height can qualitatively be explained by an interface dipole induced by the organic layer passivation [15, 17–19]. This was widely discussed in our previous study [8].

Figure 2(a) also shows the semilog *I-V* characteristic (in red) of the Al/methyl-red/*p*-InP device under light illumination. The reverse bias current of the solar cell is strongly increased by the illumination. This suggests that the carrier charges are effectively generated in the junction by illumination. This effect is due to electron–hole pair generation [4]. The increase in charge production is dependent on the difference in the electron affinities between methyl-red and *p*-InP semiconductor. The device shows a good photovoltaic behavior with a maximum open-circuit voltage V_{oc} of 0.38 V and a short-circuit current I_{sc} of 2.8 nA under 200 lux light intensity. Our result is acceptable when compared with some published previously data [31, 32]. Namely, Antohe et al. [31] reported that typical cell parameters for the ITO/CuPc/TPyP/Al photovoltaic cell illuminated in monochromatic light of 20 μW/cm^2 had the following values: $V_{oc} = 400$ mV, $J_{sc} = 135$ nA/cm^2. Also, Camaioni et al. [32] obtained a value of $J_{sc} = 30$ nAcm^{-2} for ITO/poly(C2CPDT)/Al structure under 1 mWcm^{-2} illumination.

3.2. The Capacitance and Interface Properties of the Al/Methyl-Red/p-InP Structure. Figure 2(b) shows the *C-V* characteristic of the Al/methyl-red/*p*-InP device for 500 kHz at room temperature. The inset of this figure indicates conductance-voltage (*G-V*) characteristic of the Al/methyl-red/*p*-InP device obtained from the *C-V*. By using the relationship between capacitance-voltage [23, 24], the barrier height and acceptor carrier concentration values for the Al/methyl-red/*p*-InP devices were extracted as 1.27 eV and 3.46×10^{17} cm^{-3} from linear region of its C^{-2}-*V* characteristics [8], respectively. The difference between $\Phi_b(I\text{-}V)$and $\Phi_b(C\text{-}V)$ for Al/methyl-red/*p*-InP devices originates from the different nature of the *I-V* and *C-V* measurements. Due to different nature of the *C-V* and *I-V* measurement techniques, barrier heights deduced from them are not always the same. The capacitance C is insensitive to potential fluctuations on a length scale of less than the space charge region and *C-V* method averages over the whole area and measures to describe BH. The DC current I across the interface depends exponentially on barrier height and thus sensitively on the detailed distribution at the interface [24, 33]. Additionally, the discrepancy between the barrier height values of the devices may also be explained by the existence of the interfacial layer and trap states in semiconductor [34].

A peak of the *C-V* characteristic of the OI device in Figure 2(b) gives a value of $C_{ox} = 1365$ pF that is the capacitance of the native oxide layer plus methyl-red film. The capacitance C_{ss} and conductance G_{ss} of the interface states for the device are in parallel to the capacitance of the depletion region C_{sc} and in series to interfacial layer capacitance C_{ox} [35–38]. Figures 3(a) and 3(b) show the experimental capacitance and conductance as a function of the frequency with steps of 0.04 V, respectively. The experimental *C-f* and *G-f* characteristics were simultaneously measured in the frequency range of 1 kHz-5 MHz. As can be seen from Figure 3(a), the measured capacitance decreases with an increase in the frequency. This indicates the presence of a continuous distribution of the interface states, leading to a progressive decrease of the response of the interface states to the applied ac voltage [37].

We can calculate the density distribution of the interface states from the experimental *C-f* and *G-f* measurements (the conductance method) of the Al/methyl-red/*p*-InP structure. According to Nicollian and Goetzberg [35, 36], the interface state conductance for this structure can be described as

$$G_{ss} = \frac{AqN_{ss}}{2\tau} \ln(1 + w^2\tau^2), \quad (1)$$

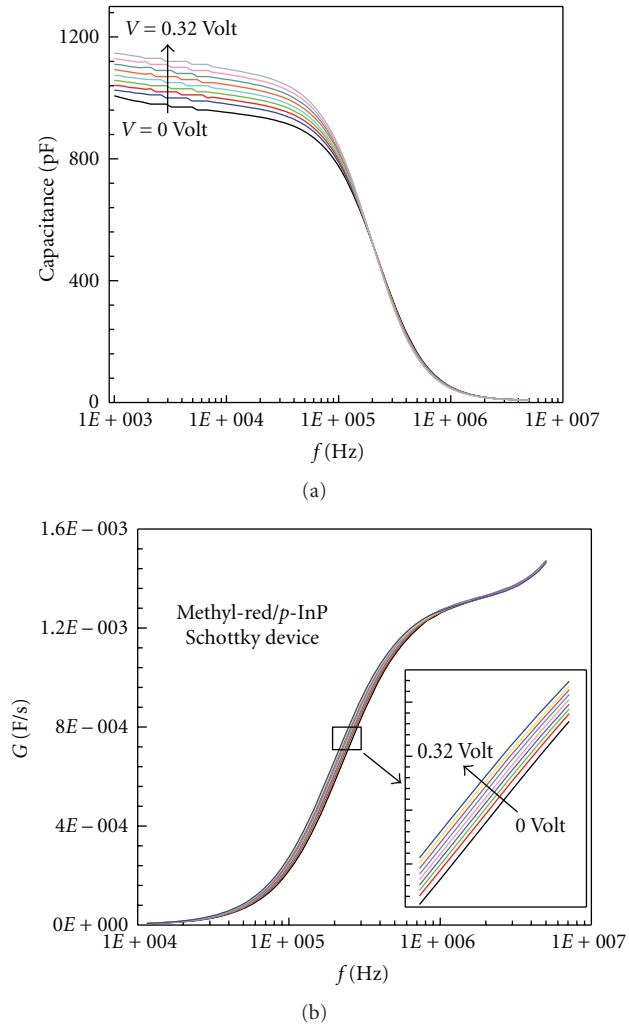

Figure 3: (a) (Color online) experimental capacitance-frequency characteristics of the Al/methyl-red/p-InP device under dark condition. (b) Experimental conductance-frequency characteristics of the Al/methyl-red/p-InP device under dark condition.

where $w = 2\pi f$ is the angular frequency, and τ is time constant of the interface states which can be written as

$$\tau = \frac{1}{\nu_{\text{th}}\sigma N_{\text{a}}} \exp\left(\frac{qV_d}{kT}\right). \tag{2}$$

N_{ss} is the interface state density, σ is the cross section of interface states, ν_{th} is the thermal velocity of carrier, and N_{a} is the doping concentration and A is the contact area.

The conductance of the interface states G_{ss} is given by [36, 37]

$$G_{\text{ss}} = \frac{C_{\text{ox}}^2 G}{(C_{\text{ox}} - C)^2 + (G/w)^2}, \tag{3}$$

where G and C are the experimental conductance and capacitance of the diode, respectively. Furthermore, the energy of the interface states E_{ss} with respect to the top of the valance band (E_{v}) at the surface of the semiconductor for a p-type semiconductor is given by [30]

$$E_{\text{ss}} - E_{\text{v}} = q\Phi_b - qV. \tag{4}$$

As explained in [25, 30, 36], the conductance method yields more accurate and reliable results about interface states. The conductance technique involves point by point determination of the density of interface states throughout the depletion region. The only contribution to conductance comes from the interface states [39–43]. The parameters such as series resistance and bulk states can generally affect the conductance at high frequency. The quantity G_{ss}/w given in Figure 4(a) was calculated from the C and G versus frequency measurements (Figures 3(a) and 3(b)) with the help of (3). The G_{ss}/w versus w behavior can be explained by the presence of an almost continuous distribution of interface state energy levels. At a given bias, the Fermi level fixes the occupancy of these interface traps levels, and a particular interface charge density will be at the InP surface which determines the time constant of the related interface states. When the a.c. signal corresponds to this time constant, the peak loss associated to the interface trap levels will occur. If the frequency is slightly different from the time constant, loses are reduced because trap levels do not respond or the response occurs at a different frequency. Therefore, the loss peak is a function of frequency. Moreover, the peak value depends on the capture rate, that is, on the interface state level occupancy that is determined by the applied bias [25, 44, 45]. The curves go through maxima at $w\tau = 1.98$ with values of $(G_{\text{ss}}/w)_{\text{max}} = 0.40qAN_{\text{ss}}$ [35, 36]. The ordinates and frequencies of the maxima yield therefore density of the interface states and their time constant, τ. Then, the dependence of N_{ss} and τ on the bias was converted to a function of E_{ss} using (4). Figure 4(b) shows the energy distribution curves of the interface states and their time constants obtained from the experimental G_{ss}/w versus w characteristics of the Al/methyl-red/p-InP structure at room temperature. The interface state densities and their relaxation times have ranged from $2.96 \times 10^{12}\,\text{cm}^{-2}\,\text{eV}^{-1}$ and 4.96×10^{-6} seconds at (1.11-E_{v}) eV to $5.19 \times 10^{12}\,\text{cm}^{-2}\,\text{eV}^{-1}$ and 9.39×10^{-6} seconds at (0.79-E_{v}) eV, respectively. As can be seen from Figure 4(b), both the interface state density and the relaxation time of the interface states decrease with bias voltage. Aydogan et al. [46] found that the deposition of polymers on to the inorganic semiconductor can generate large number of interface states at the semiconductor surface, which strongly influence the properties of the PANI/p-Si/Al structure. Çakar et al. [47] have determined interface properties of Au/PYR-B/p-Si/Al contact. They [47] have found that the interface-state density values vary from 4.21×10^{13} to $3.82 \times 10^{13}\,\text{cm}^{-2}\,\text{eV}^{-1}$. In another study, Aydin et al. [23] have investigated the interface-state density properties of the Sn/methyl-red/p-Si/Al diode, and interface state density was found to vary from $1.68 \times 10^{12}\,\text{cm}^{-2}\,\text{eV}^{-1}$ to $1.80 \times 10^{12}\,\text{cm}^{-2}\,\text{eV}^{-1}$. The interface-state density of the Al/methyl-red/p-InP diode is consistent with those of above mentioned diodes.

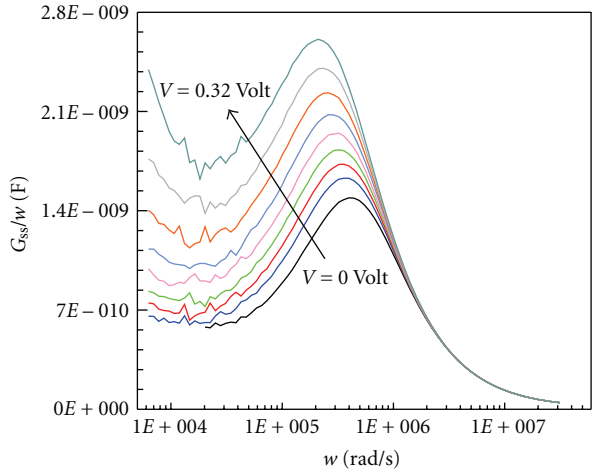

(a)

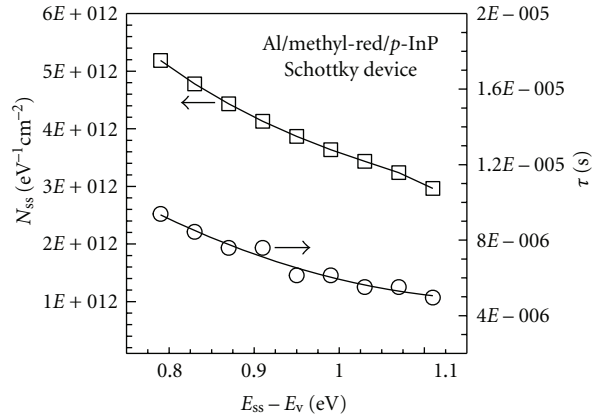

(b)

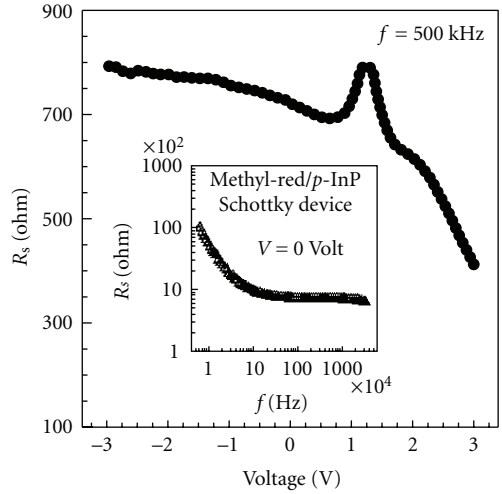

(c)

Figure 4: (a) (Color online) G_{ss}/w versus w characteristics obtained from the experimental forward bias capacitance and conductance versus frequency measurements of the Al/methyl-red/p-InP structure in dark. (b) Energy distribution curves of the interface states and their time constants obtained from the experimental G_{ss}/w versus w characteristics for the Al/methyl-red/p-InP structure in dark. (c) The R_s-V characteristic of the Al/methyl-red/p-InP device for 500 kHz frequency in dark (inset represents the R_s-f characteristic of that for 0 volt in dark).

The frequency and voltage dependent series resistances of the device can be calculated from the experimental C-V-f measurements as [36]

$$R_s = \frac{G}{G^2 + (wC)^2}, \tag{5}$$

where C is measured capacitance, and G is conductance values. The series resistance of Al/methyl-red/p-InP structure as a function of the voltage was calculated by using (5). Figure 4(c) depicts the voltage dependency of the series resistance for 500 kHz frequency. As seen from Figure 4(c), the R_s decreases with the increasing bias voltage by giving a peak at about 1.4 V. This behavior shows that the carriers have enough energy to escape from the traps located between metal and semiconductor interface in the band gap of InP [48]. Also, the series resistance of the device as a function of the frequency was calculated by using (5). The inset of Figure 4(c) shows the frequency dependency of the series resistance for zero Volt. As can clearly seen from the figure, the series resistance rapidly decreases with increase in frequency at low frequencies and then remains nearly constant. The voltage and frequency dependency of the R_s is attributed to the particular distribution of interface density states and interface layer [48].

4. Conclusion

Electronic and photovoltaic properties of the Al/methyl-red/p-InP heterojunction diode have been investigated. The ideality factor n and barrier height Φ_b values of the diode in dark were found to be 2.02 and 1.11 eV, respectively. The device is a photodiode with electronic parameters, a maximum open-circuit voltage of 0.38 V and a short-circuit current of 2.8 nA under 200 lx light intensity. The barrier height and acceptor carrier concentration values for the Al/methyl-red/p-InP solar cell device were extracted as 1.27 eV and 3.46×10^{17} cm^{-3} from linear region of C^{-2}-V characteristics, respectively. The difference in the barrier heights obtained from I-V and C-V measurements for Al/methyl-red/p-InP device was attributed the different nature of the I-V and C-V measurements. In addition, the energy distribution plots of the interface states and their time constants were calculated from the experimental conductance properties of the Al/methyl-red/p-InP device at room temperature. It was seen that both the interface state density and the relaxation time of the interface states obtained from capacitive measurements decreased with bias voltage.

Acknowledgment

The author wishes to thank Professor Dr. A.Turut, from Ataturk University, Turkey, for his valuable help and critical reading of the manuscript.

References

[1] J. Lee, S. S. Kim, K. Kim, J. H. Kim, and S. Im, "Correlation between photoelectric and optical absorption spectra of thermally evaporated pentacene films," *Applied Physics Letters*, vol. 84, no. 10, pp. 1701–1703, 2004.

[2] T. Kurata, H. Koezuka, S. Tsunoda, and T. Ando, "Metal/conductive-polymer junction: an In/poly(*N*-methylpyrrole) diode with a tunnel Schottky junction," *Journal of Physics D*, vol. 19, no. 4, pp. L57–L60, 1986.

[3] K. Tada, M. Wada, and M. Onoda, "A polymer Schottky diode carrying a chimney for selective doping," *Journal of Physics D*, vol. 36, no. 17, pp. L70–L73, 2003.

[4] F. Yakuphanoglu, "Electronic and photovoltaic properties of Al/p-Si/copper phthalocyanine photodiode junction barrier," *Solar Energy Materials and Solar Cells*, vol. 91, no. 13, pp. 1182–1186, 2007.

[5] B. Johnev and K. Fostiropoulos, "Zinc-phthalocyaninetetraphosphonic acid as a novel transparent-conducting-oxide passivation for organic photovoltaic devices," *Solar Energy Materials and Solar Cells*, vol. 92, no. 4, pp. 393–396, 2008.

[6] A. Türüt and F. Koleli, "Semiconductive polymer-based Schottky diode," *Journal of Applied Physics*, vol. 72, no. 2, pp. 818–819, 1992.

[7] S. Aydogan, M. Saglam, and A. Türüt, "The temperature dependence of current-voltage characteristics of the Au/Polypyrrole/p-Si/Al heterojunctions," *Journal of Physics Condensed Matter*, vol. 18, no. 9, pp. 2665–2676, 2006.

[8] Ö. Güllü, A. Türüt, and S. Asubay, "Electrical characterization of organic-on-inorganic semiconductor Schottky structures," *Journal of Physics: Condensed Matter*, vol. 20, no. 4, Article ID 045215, 2008.

[9] S. R. Forrest and P. H. Schmidt, "Semiconductor analysis using organic-on-inorganic contact barriers. I. Theory of the effects of surface states on diode potential and ac admittance," *Journal of Applied Physics*, vol. 59, no. 2, pp. 513–525, 1986.

[10] S. R. Forrest, M. L. Kaplan, and P. H. Schmidt, "Semiconductor analysis using organic-on-inorganic contact barriers. II. Application to InP-based compound semiconductors," *Journal of Applied Physics*, vol. 60, no. 7, pp. 2406–2418, 1986.

[11] M. Çakar, C. Temirci, and A. Türüt, "The Schottky barrier height of the rectifying Cu/pyronine-B/p-Si, Au/pyronine-B/p-Si, Sn/pyronine-B/p-Si and Al/pyronine-B/p-Si contacts," *Synthetic Metals*, vol. 142, no. 1–3, pp. 177–180, 2004.

[12] M. A. Ebeoglu, T. Kilicoglu, and M. E. Aydin, "Low- and high-frequency C-V characteristics of the contacts formed by adding a solution of the nonpolymeric organic compound on p-type Si substrate," *Physica B*, vol. 395, no. 1-2, pp. 93–97, 2007.

[13] M. M. El-Nahass, K. F. Abd-El-Rahman, A. A. M. Farag, and A. A. A. Darwish, "Photovoltaic properties of NiPc/p-Si (organic/inorganic) heterojunctions," *Organic Electronics: Physics, Materials, Applications*, vol. 6, no. 3, pp. 129–136, 2005.

[14] M. M. El-Nahass, H. M. Zeyada, K. F. Abd-El-Rahman, and A. A. A. Darwish, "Fabrication and characterization of 4-tricyanovinyl-*N*,*N*-diethylaniline/p-silicon hybrid organic-inorganic solar cells," *Solar Energy Materials and Solar Cells*, vol. 91, no. 12, pp. 1120–1126, 2007.

[15] T. Kampen, A. Schuller, D. R. T. Zahn, et al., "Schottky contacts on passivated GaAs(100) surfaces: barrier height and reactivity," *Applied Surface Science*, vol. 234, no. 1–4, pp. 341–348, 2004.

[16] D. R. T. Zahn, T. U. Kampen, and H. Mendez, "Transport gap of organic semiconductors in organic modified Schottky contacts," *Applied Surface Science*, vol. 212-213, pp. 423–427, 2003.

[17] A. R. Vearey-Roberts and D. A. Evans, "Modification of GaAs Schottky diodes by thin organic interlayers," *Applied Physics Letters*, vol. 86, no. 7, Article ID 072105, 3 pages, 2005.

[18] A. Bolognesi, A. Di Carlo, P. Lugli, T. Kampen, and D. R. T. Zahn, "Experimental investigation and simulation of hybrid organic/inorganic Schottky diodes," *Journal of Physics: Condensed Matter*, vol. 15, no. 38, pp. S2719–S2728, 2003.

[19] T. U. Kampen, S. Park, and D. R. T. Zahn, "Barrier height engineering of Ag/GaAs(100) Schottky contacts by a thin organic interlayer," *Applied Surface Science*, vol. 190, no. 1–4, pp. 461–466, 2002.

[20] C. H. Chen and I. Shih, "Hybrid organic on inorganic semiconductor heterojunction," *Journal of Materials Science: Materials in Electronics*, vol. 17, no. 12, pp. 1047–1053, 2006.

[21] R. K. Gupta and R. A. Singh, "Junction properties of Schottky diode based on composite organic semiconductors: polyaniline-polystyrene system," *Journal of Polymer Research*, vol. 11, no. 4, pp. 269–273, 2005.

[22] T. Kilicoglu, M. E. Aydin, and Y. S. Ocak, "The determination of the interface state density distribution of the Al/methyl-red/p-Si Schottky barrier diode by using a capacitance method," *Physica B*, vol. 388, no. 1-2, pp. 244–248, 2007.

[23] M. E. Aydin and A. Türüt, "The electrical characteristics of Sn/methyl-red/p-type Si/Al contacts," *Microelectronic Engineering*, vol. 84, no. 12, pp. 2875–2882, 2007.

[24] E. H. Rhoderick and R. H. Williams, *Metal-Semiconductor Contacts*, Clarendon, Oxford, UK, 2nd edition, 1988.

[25] S. M. Sze, *Physics of Semiconductor Devices*, John Wiley & Sons, New York, NY, USA, 2nd edition, 1981.

[26] R. F. Schmitsdorf, T. U. Kampen, and W. Monch, "Explanation of the linear correlation between barrier heights and ideality factors of real metal-semiconductor contacts by laterally nonuniform Schottky barriers," *Journal of Vacuum Science and Technology B*, vol. 15, no. 4, pp. 1221–1226, 1997.

[27] W. Monch, "Barrier heights of real Schottky contacts explained by metal-induced gap states and lateral inhomogeneities," *Journal of Vacuum Science and Technology B*, vol. 17, no. 4, pp. 1867–1876, 1999.

[28] R. T. Tung, "Electron transport at metal-semiconductor interfaces: general theory," *Physical Review B*, vol. 45, no. 23, pp. 13509–13523, 1992.

[29] G. M. Vanalme, L. Goubertt, R. L. Van Meirhaeghe, F. Cardon, and P. Van Daele, "Ballistic electron emission microscopy study of barrier height inhomogeneities introduced in Au/III-V semiconductor Schottky barrier contacts by chemical pretreatments," *Semiconductor Science and Technology*, vol. 14, no. 9, pp. 871–877, 1999.

[30] M. Çakar, N. Yildirim, Ş. Karataş, C. Temirci, and A. Türüt, "Current-voltage and capacitance-voltage characteristics of Sn/rhodamine- 101*n*-Si and Sn/rhodamine- 101*p*-Si Schottky barrier diodes," *Journal of Applied Physics*, vol. 100, no. 7, Article ID 074505, 2006.

[31] S. Antohe, "Electrical and photoelectrical properties of the single-, and multilayer organic photovoltaic cells," *Journal of Optoelectronics and Advanced Materials*, vol. 2, no. 5, pp. 498–514, 2000.

[32] N. Camaioni, G. Casalbore-Miceli, G. Beggiato, M. Cristani, and C. Summonte, "Photoelectrical characterization of

Schottky junctions between poly(4h-cyclopenta[2,1-*b*:3,4-*b*′]dithiophene) and aluminum: effect of hexadecyl groups in 4 position," *Thin Solid Films*, vol. 366, no. 1-2, pp. 211–215, 2000.

[33] J. H. Werner and H. H. Guttler, "Barrier inhomogeneities at Schottky contacts," *Journal of Applied Physics*, vol. 69, no. 3, pp. 1522–1533, 1991.

[34] H. C. Card and E. H. Rhoderick, "Studies of tunnel MOS diodes I. Interface effects in silicon Schottky diodes," *Journal of Physics D*, vol. 4, no. 10, pp. 1589–1601, 1971.

[35] E. H. Nicollian and A. Goetzberger, "The Si-SiO_2 interface—electrical properties as determined by the metal-insulator-silicon conductance technique," *Bell System Technical Journal*, vol. 46, pp. 1055–1163, 1967.

[36] E. H. Nicollian and J. R. Brews, *MOS (Metal Oxide Semiconductor) Physics and Technology*, John Wiley & Sons, New York, NY, USA, 1982.

[37] J. Fernandez, P. Godignon, S. Berberich, J. Rebollo, G. Brezeanu, and J. Millan, "High frequency characteristics and modelling of P-type 6H-silicon carbide MOS structures," *Solid-State Electronics*, vol. 39, no. 9, pp. 1359–1364, 1996.

[38] M. Biber, M. Çakar, and A. Türüt, "The effect of anodic oxide treatment on n-GaAs Schottky barrier diodes," *Journal of Materials Science: Materials in Electronics*, vol. 12, no. 10, pp. 575–579, 2001.

[39] M. E. Yacoubi, R. Evrard, N. D. Nguyen, and M. Schmeits, "Electrical conduction by interface states in semiconductor heterojunctions," *Semiconductor Science and Technology*, vol. 15, no. 4, pp. 341–348, 2000.

[40] E. K. Evangelou, N. Konofaos, M. R. Craven, W. M. Cranton, and C. B. Thomas, "Characterization of the $BaTiO_3$/p-Si interface and applications," *Applied Surface Science*, vol. 166, no. 1, pp. 504–507, 2000.

[41] O. L. Blajiev, T. Breugelmans, R. Pintelon, and A. Hubin, "Improvement of the impedance measurement reliability by some new experimental and data treatment procedures applied to the behavior of copper in neutral chloride solutions containing small heterocycle molecules," *Electrochimica Acta*, vol. 51, no. 8-9, pp. 1403–1412, 2006.

[42] N. Konofaos and E. K. Evangelou, "Electrical characterization of the SiON/Si interface for applications on optical and MOS devices," *Semiconductor Science and Technology*, vol. 18, no. 1, pp. 56–59, 2003.

[43] S. Kochowski, B. Paszkiewicz, and R. Paszkiewicz, "Some effects of $(NH_4)_2S_x$ treatment of n-GaAs surface on electrical characteristics of metal-SiO_2-GaAs structures," *Vacuum*, vol. 57, no. 2, pp. 157–162, 2000.

[44] M. C. Lonergan and F. E. Jones, "Calculation of transmission coefficients at nonideal semiconductor interfaces characterized by a spatial distribution of barrier heights," *Journal of Chemical Physics*, vol. 115, no. 1, pp. 433–445, 2001.

[45] S. Karatas and A. Türüt, "The determination of interface state energy distribution of the H-terminated Zn/p-type Si Schottky diodes with high series resistance by the admittance spectroscopy," *Vacuum*, vol. 74, no. 1, pp. 45–53, 2004.

[46] S. Aydogan, M. Saglam, and A. Türüt, "Some electrical properties of polyaniline/p-Si/Al structure at 300 K and 77 K temperatures," *Microelectronic Engineering*, vol. 85, no. 2, pp. 278–283, 2008.

[47] M. Çakar, N. Yıldırım, H. Doğan, and A. Türüt, "The conductance and capacitance-frequency characteristics of Au/pyronine-B/p-type Si/Al contacts," *Applied Surface Science*, vol. 253, no. 7, pp. 3464–3468, 2007.

[48] F. Parlaktürk, S. Altindal, A. Tataroğlu, M. Parlak, and A. Agasiev, "On the profile of frequency dependent series resistance and surface states in Au/$Bi_4Ti_3O_{12}$/SiO_2/n-Si(MFIS) structures," *Microelectronic Engineering*, vol. 85, no. 1, pp. 81–88, 2008.